(2)

AD-A154 228

AD

AD-E401 333

TECHNICAL REPORT ARLCD-TR-85005

DESIGN AND TESTING OF A PULSED CURRENT TRANSFORMER

ALEX E. ZIELINSKI

APRIL 1985

U.S. ARMY ARMAMENT RESEARCH AND DEVELOPMENT CENTER

LARGE CALIBER WEAPON SYSTEMS LABORATORY

DOVER, NEW JERSEY

APPROVED FOR PUBLIC RELEASE; DISTRIBUTION UNLIMITED.

85 05 13 054

UNCLASSIFIED

SECURITY CLASSIFICATION OF THIS PAGE (When Data Entered)

REPORT DOCUMENTATION PAGE

READ INSTRUCTIONS BEFORE COMPLETING FORM

1. REPORT NUMBER: Technical Report ARLCD-TR-85005	2. GOVT ACCESSION NO.: AD-A154 228
3. RECIPIENT'S CATALOG NUMBER	
4. TITLE (and Subtitle): DESIGN AND TESTING OF A PULSED CURRENT TRANSFORMER	5. TYPE OF REPORT & PERIOD COVERED: Test July 1984—December 1984
	6. PERFORMING ORG. REPORT NUMBER
7. AUTHOR(s): Alex E. Zielinski	8. CONTRACT OR GRANT NUMBER(s)
9. PERFORMING ORGANIZATION NAME AND ADDRESS: ARDC, LCWSL Applied Sciences Div (SMCAR-LCA-G) Dover, NJ 07801-5001	10. PROGRAM ELEMENT, PROJECT, TASK AREA & WORK UNIT NUMBERS
11. CONTROLLING OFFICE NAME AND ADDRESS: ARDC, TSD STINFO Div (SMCAR-TSS) Dover, NJ 07801-5001	12. REPORT DATE: April 1985
	13. NUMBER OF PAGES: 30
14. MONITORING AGENCY NAME & ADDRESS (if different from Controlling Office)	15. SECURITY CLASS. (of this report): Unclassified
	15a. DECLASSIFICATION/DOWNGRADING SCHEDULE

16. DISTRIBUTION STATEMENT (of this Report)

Approved for public release; distribution unlimited.

17. DISTRIBUTION STATEMENT (of the abstract entered in Block 20, if different from Report)

18. SUPPLEMENTARY NOTES

19. KEY WORDS (Continue on reverse side if necessary and identify by block number)

Railgun
Pulse transformer
Current multiplication
Capacitor bank
Skin depth
Barrel test section
Electromagnetics
Inductance gradient

20. ABSTRACT (Continue on reverse side if necessary and identify by block number)

A pulsed current transformer was built and tested. Data substantiating the theoretical model was obtained.

The four turn, coaxial geometry transformer had a mean radius of 12 inches. It used copper tubing for the secondary and number 6 gage wire for the primary. Under short circuit conditi‹- , the time-to-peak current was 70 microseconds and a time averaged turns ratio of 3.75 was produced by the transformer.

(cont)

DD FORM 1 JAN 73 1473 EDITION OF 1 NOV 65 IS OBSOLETE

UNCLASSIFIED

SECURITY CLASSIFICATION OF THIS PAGE (When Data Entered)

20. ABSTRACT (cont)

The theoretical model yielded an input inductance of 1.93 microhenries while the high frequency measurement yielded 1.66 microhenries.

By increasing the secondary wall thickness, this device will be useful in electromagnetically stressing barrel test sections at the megampere level.

CONTENTS

TABLES

FIGURES

INTRODUCTION

The concept of accelerating particles with a parallel rail, electromagnetic launcher has been known for many years. Basic equations of motion ($m\dot{v} = 1/2\ L'I^2$) show that high currents are required for high velocities. These high currents produce high pressures which must be withstood by the launch structure. If launcher barrels are to be designed for high velocity applications, the modeling of containment structures has to be performed in the presence of large magnetic fields.

Capacitors are a common energy store for pulsed power applications. Because of the rapid discharge rate of the capacitor, it has to be connected to an inductor to provide power conditioning. A coaxial pulse transformer provides the appropriate current output and substantially reduces the external magnetic field associated with pulsed coils.

There are five 50 kilojoule (100 KA) Maxwell capacitor banks at the Armament Research and Development Center (ARDC). By connecting a five-turn pulse transformer to each bank, currents on the order of 2 megamperes can be generated to electromagnetically stress barrel test sections to twice their rated pressure (10 Kbar).

In order to model the various subcomponents (pulse transformer, barrels, breech plates), a small scale capacitor bank was built. This pulsed power supply was used in connection with a model pulse transformer to conduct tests to verify the pulse transformer model.

DISCUSSION

The load switch used in the completed power supply (fig. 1) was an International Rectifier 151RA100. A plot of the silicon controlled rectifier (SCR) fuzing current versus pulse width is shown in figure A-1 of the appendix. The maximum dI/dt rating is 3×10^8 amperes per second. The fast rise time gate pulse which the SCR requires at this level was accomplished with a 555-timer circuit (fig. A-2). A 12 volt, 15-microsecond pulse is delivered to a Darlington pair where a 1:2 pulse transformer supplies approximately 10 watts of power to the SCR gate. This 555-output pulse is also optically coupled to another 555 circuit which stretches the pulse width and establishes a reliable, isolated scope trigger (fig. A-3). The 1306-microfarad storage capacitor is charged from a high voltage power supply through a relay. A 120-VAC relay (Radio Shack 275-003) was found to open and close reliably up to 800 VDC. Once the pulse button is pushed, there is a 3-second delay before the gate pulse is initiated to the SCR.

The output buss is a parallel plate type for low inductance. A crowbar diode (250 A, 1 KV) was placed across the capacitor to prevent voltage reversal.

Pulse Transformer

The model transformer was built from off-the-shelf laboratory materials. The primary winding was made from no. 6 gage stranded copper wire; the secondary winding, from 3/8-inch outer diameter copper water tubing; and the connection bars, from 2-inch by 3/4-inch copper stock. The tubing was bent on a wooden form and soldered to the connection bars, resulting in a mean radius (r) of 12 inches. The primary cable was then pulled through the secondary tubing. The insulator between the connection bars was made from 0.035-inch phenolic. The connection bars were clamped together with 3/8-inch phenolic strips, and plexiglass spacers were used to keep an even distance between windings. The assembled model and circuit diagram are shown in figure 2.

Theoretical Model

Writing the derivative of the energy equation in an LRC circuit, we get

$$\frac{d}{dt}\left(1/2\ L_1\ I_1{}^2 + 1/2\ L_2\ I_2{}^2\right) + \frac{d}{dt}\int B^2/2u\ dv + \frac{d}{dt}\left(1/2\ Q^2/C\right) +$$

$$I_1{}^2\ R_1 + I_2{}^2\ R_2 = 0 \qquad (1)$$

The subscripts denote primary "1" and secondary "2" side parameters; the term involving $\int B^2/2u\ dv$ accounts for the inductance of the transformer where u is taken to be the permeability of a vacuum. The primary winding resistance can be included in the R_1 term. In this analysis the power dissipated in the secondary has been neglected. The geometry for the pulse transformer is shown in figure A-4 where the uniform current density in the primary and flux exclusion in the secondary tubing (i.e., a thin current sheet) is assumed.

The B field in the primary winding is found from $\oint B \cdot dl = \oint J \cdot da$. For $0<\xi<a$, J is uniform and equal to $I/\pi a^2$. Integrating J over the surface $\pi\xi^2$, results in $B = uI\xi/2\pi a^2$. Therefore, $B^2/2u = I^2\xi^2 u/8\pi^2 a^4$. In the region $a<\xi<b$, $B = uI/2\pi\xi$ and $B^2/2u = I^2 u/\pi^2 8\xi^2$. Integrating the magnetic pressure for the two regions over the volume element $(2\pi r)\ (2\pi\xi)\ (d\xi)$, the total stored magnetic energy per turn of the coaxial pulse transformer as $I^2 ur\ [0.25 + \ln(b/a)]/2$ is obtained.

The inductance due to the output connection bars (of height, h, and separation, W) can be calculated by use of a thin current sheet approximation. The inductance gradient for this geometry is given* as

$$L_b' = \frac{\mu}{\pi}\left[\frac{1}{2}\ln(\alpha^2 + 1) - \frac{1}{2}\alpha^2 \ln(1/\alpha^2 + 1) + 2\alpha \tan^{-1}(1/\alpha)\right];$$

where $\alpha = W/h$. Since each secondary tube contributes a current I_1, the total output current ($I_2 = NI_1$) is obtained after the Nth winding. The magnetic energy can be expressed as

$$(0.5\, L_b' X) \sum_{n=1}^{N-1} (I_1 n)^2$$

where X is the winding spacing of the secondary tubes. The inductance after the N-1 turn is included in the load term (N^2L_2).

Expanding equation 1 we get

$$L_1 I_1 \dot{I}_1 + N^2 L_2 I_1 \dot{I}_1 + Nu I_1 \dot{I}_1 r\, [0.25 + \ln(b/a)] + L_b I_1 \dot{I}_1 \sum_{n=1}^{N-1} (n^2) +$$
$$QI_1/C + I_1^2 R_1 + N^2 I_1^2 R_2 = 0$$

where $I_2 = NI_1$.

The following equation is obtained by simplifying terms:

$$L_1 \dot{I}_1 + N^2 L_2 \dot{I}_1 + Nu \dot{I}_1 r\, [0.25 + \ln(b/a)] + \dot{I}_1 L_b \sum_{n=1}^{N-1} (n^2) + Q/C + I_1 R_1 +$$
$$N^2 I_1 R_2 = 0$$

Combining terms and again taking the derivative

$$\left[L_1 + N^2 L_2 + NK + L_b \sum_{n=1}^{N-1} (n^2)\right] \ddot{I}_1 + (R_1 + N^2 R_2)\, \dot{I}_1 + I_1/C = 0$$

---

* J. A. Bennett, "Some notes on the Calculation of Railgun Inductance," Information Report ASD 10-82, June 1979.

where NK = Nur [0.25 + ln(b/a)] is the total inductance of the pulse transformer referred to the primary side. Solving the differential equation for the under-damped case

$$I_1(t) = (V_c/wL)\ \mathrm{EXP}(-R\ t/2\ L)\ \sin(w\ t)$$

where

$$L = L_1 + N^2L_2 + NK + L_b \sum_{n-1}^{N-1} (n^2)$$

$$R = R_1 + N^2R_2$$

Vc = initial capacitor voltage and

$$w = \sqrt{[1/LC - (R/2\ L)^2]}$$

In this analysis we have assumed that the times of interest are short; the B field for $\xi>b$ is set equal to zero. In other words, the transient skin depth $(\sqrt{\pi t/\mu\sigma})$ is considered much less than the thickness of the secondary tubing.

Experiments

Description

There were two sets of tests performed: where the time-to-peak current was 100 microseconds, and another where it was 70 microseconds.

Because the secondary tubing is thin (0.035 in.), it is understood that this is not an optimum design (number of turns equal to the current multiplication factor). However, if the times-to-peak current are short enough, the model can be corroborated.

For the first set of tests the load was inductive. Impedance measurements of the following elements (table 1) were taken with a Hewlett Packard LRC bridge (model 4274A): (1) leads to the pulse transformer, (2) input of the pulse transformer with the load coil, and (3) load coil. The diagnostics consisted of measuring the capacitor voltage, primary voltage at the pulse transformer input, primary $\dot{I}_1$, and secondary $\dot{I}_2$. Initial capacitor voltages were in the range of 200 to 450 volts. Six tests were performed with each yielding similar waveforms. A typical test discharge with the load coil connected is shown in figure 3.

The second set of tests involved the use of a 10-mil-thick copper zirconium foil as the load (short circuit) and shortening the leads to the pulse transformer.

The inductance and resistance at the pulse transformer input were measured at various frequencies using the LRC bridge. These values (fig. 4) were obtained with the secondary shorted. The diagnostics consisted of measuring the primary voltage at the pulse transformer input, the primary $\dot{I}_1$, the voltage across the foil short, and the secondary $\dot{I}_2$. The voltage across the short was measured using a coaxial type probe (fig. A-5). The Rogowski coils had a rise time of 10 microseconds.

Because of the lower input inductance (shorted secondary), the capacitor voltage was kept below a level of 300 volts so as not to exceed the dI/dt rating of the SCR. A typical test discharge is shown in figure 5.

Results

The six discharge tests with the load coil connected produced current rise times of 100 microseconds. Using the voltage and $\dot{I}_1$ waveforms along with the impedance bridge measurements in table 1 (at a frequency of 2.5 kHz), the internal inductance and resistance of the capacitor bank were found to be 0.44 microhenries and 36 milliohms, respectively. These values are due to the SCR. Time-averaged values of the input inductance and resistance of the pulse transformer with the load coil attached were found to be 4.25 microhenries and 23.36 milliohms. Under these load conditions, the bridge measurements at 2.5 kHz were 4.33 microhenries and 24.2 milliohms, respectively. The error between the data analysis and the bridge measurements is 1.8% for the inductance and 3.4% for the resistance.

The second set of tests used a 10-mil-thick copper zirconium foil as the load. This provided the inductance and resistance of the transformer since $N^2L_{(foil)}$ and $N^2R_{(foil)}$ were assumed to be much less than the short circuit inductance and resistance of the pulse transformer measured with the LRC bridge (fig. 4). The voltage and $\dot{I}_1$ waveforms yielded the pulse transformer inductance and resistance which are plotted as a function of time (fig. 6). The ratio of currents (I_2/I_1), equal to the turns ratio (N), is plotted as a function of time for the two load conditions tested (fig. 7).

RESULTS

A primary current-rise time of 70 microseconds yielded an effective time-averaged turns ratio of 3.75, while the 100-microsecond rise time yielded an effective time-averaged turns ratio of 3.0. A current multiplication factor (N) less than 4 is obtained solely due to the magnetic field diffusing out of the secondary tubing.

The inductance and resistance of the pulse transformer behave as expected. For short times ($t < 20$ microseconds), the value of the inductance is close to the model prediction: 1.72 microhenries measured from data; 1.66 microhenries measured at 100 kHz with the LRC bridge, and 1.93 microhenries calculated. The resistance is initially high because of the small area of current penetration. As time progresses, current diffuses into conductors, and the resistance approaches a constant value. The inductance increases because $\int B^2/2u \; dv$ increases.

CONCLUSIONS

It is possible to determine secondary load currents for pulse power applications from the basic model for the pulse transformer. For the LRC circuit considered, the dominant circuit parameter is the inductance term. Therefore, if greater accuracy is needed, the diffusion problem can be solved to include the power dissipated in the secondary ($\int J^2/\sigma dv$).

Currently, ARDC and the University of Texas at Austin are building five, five turn, high-current pulse transformers to be used in conjunction with the five ARDC Maxwell banks. In this design, the secondary is made from 1/4-inch-walled aluminum pipe (schedule 80). Each of the five new transformers is expected to yield an effective turns ratio of 5.

Table 1. Impedance measurements

Frequency kilohertz	Inductance (microhenries)	Resistance (milliohms)
	Leads	
1	0.602	4.3
4	0.582	5.32
10	0.542	7.64
	Load Coil	
1	0.185	0.57
4	0.179	0.69
10	0.175	0.88
	Pulse Transformer Input	
1	5.38	25.42
4	4.76	32.7
10	4.51	45.7

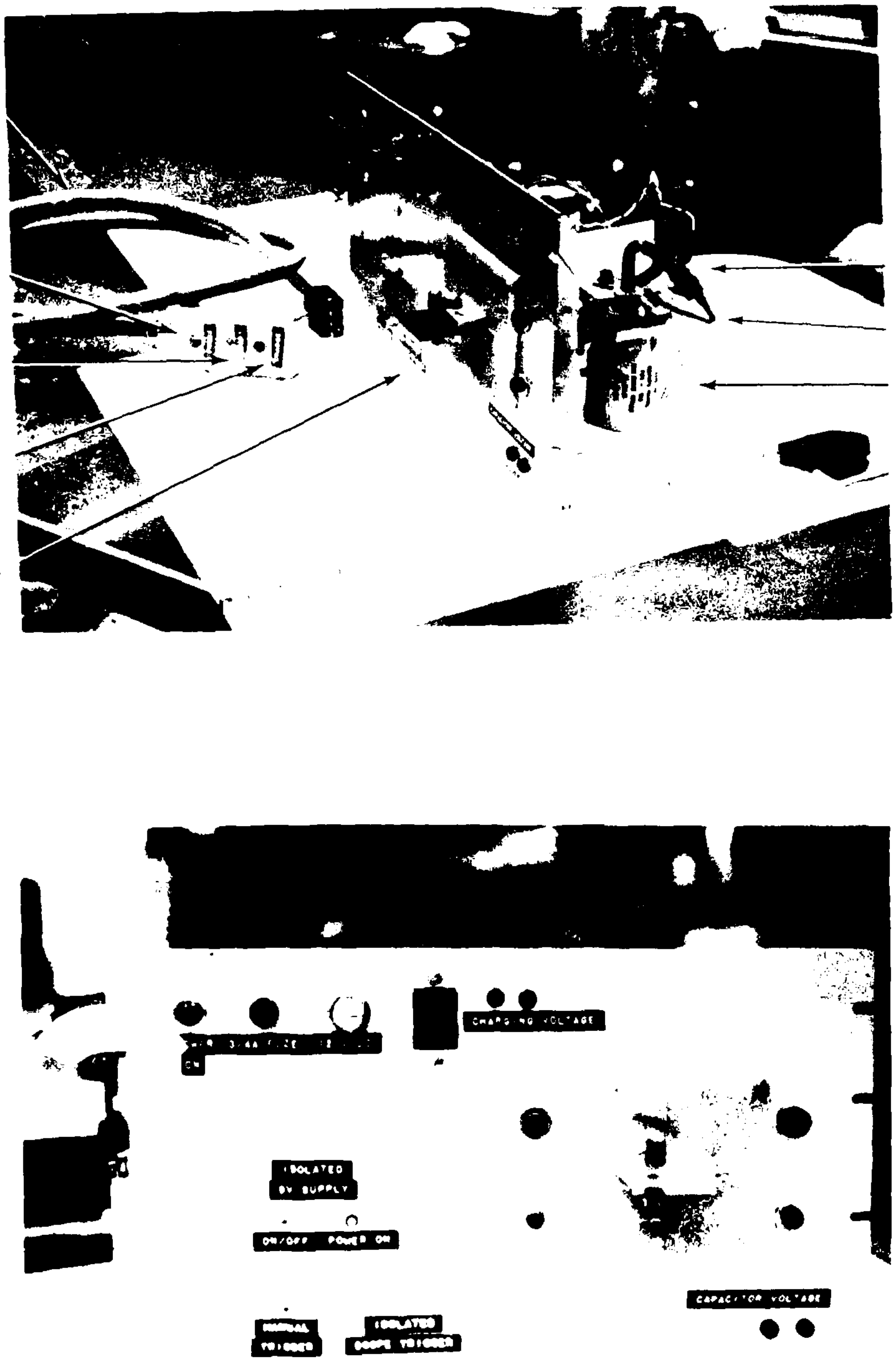

Figure 1. Capacitor bank

mmander
S. Army Armament, Munitions and Chemical Command
TN: AMSMC-LEP-L
ck Island, IL 61299-6000

rector
S. Army TRADOC Systems Analysis Activity
'TN: ATAA-SL
ite Sands Missile Range, NM 88002

DISTRIBUTION LIST

Commander
Armament Research and Development Center
U.S. Army Armament, Munitions and Chemical Command
ATTN: SMCAR-TSS (5)
SMCAR-LCA-G (10)
Dover, NJ 07801-5001

Commander
U.S. Army Armament, Munitions and Chemical Command
ATTN: AMSMC-GCL(D)
Dover, NJ 07801-5001

Administrator
Defense Technical Information Center
ATTN: Accessions Division (12)
Cameron Station
Alexandria, VA 22314

Director
U.S. Army Materiel Systems Analysis Activity
ATTN: DRXSY-MP
Aberdeen Proving Ground, MD 21005-5066

Commander
Chemical Research and Development Center
U.S. Army Armament, Munitions and Chemical Command
ATTN: SMCCR-SPS-IL
Aberdeen Proving Ground, MD 21010-5423

Commander
Chemical Research and Development Center
U.S. Army Armament, Munitions and Chemical Command
ATTN: SMCCR-RSP-A
Aberdeen Proving Ground, MD 21010-5423

Director
Ballistic Research Laboratory
ATTN: AMXBR-OD-ST
Aberdeen Proving Ground, MD 21005-5066

Chief
Benet Weapons Laboratory, LCWSL
Armament Research and Development Center
U.S. Army Armament, Munitions and Chemical Command
ATTN: SMCAR-LCB-TL
Watervliet, NY 12189-5000

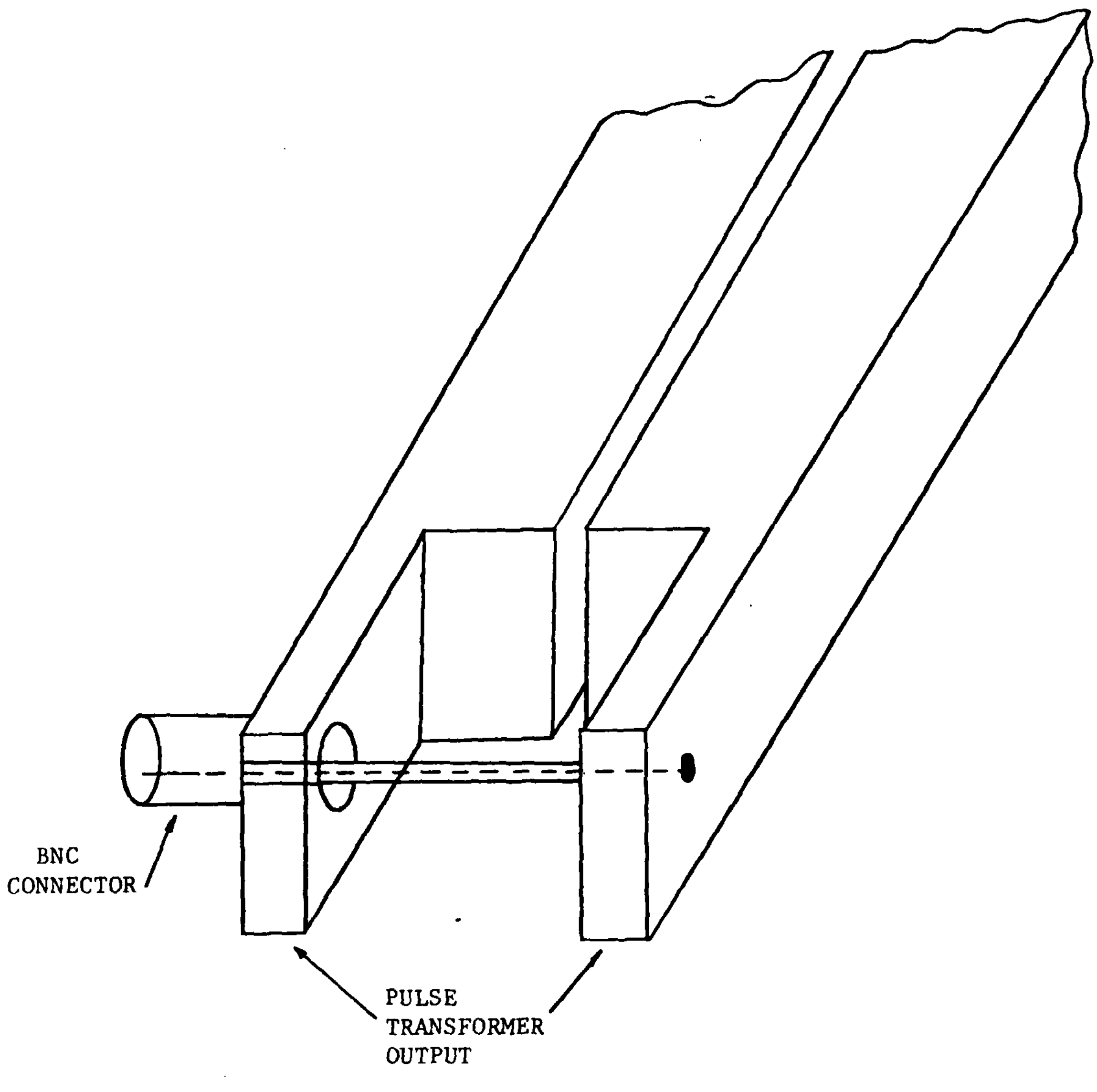

Figure A-5. Coaxial voltage probe

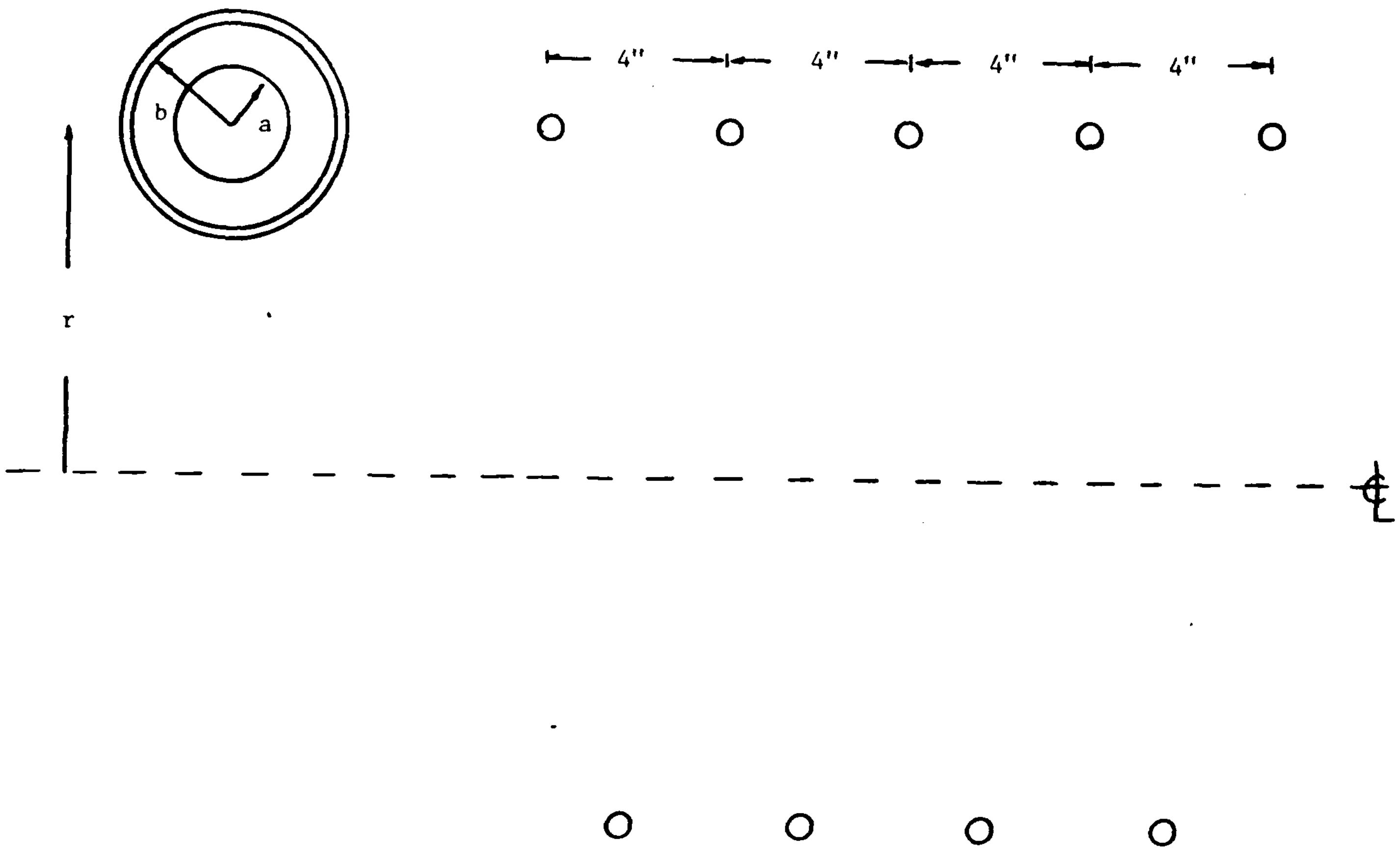

Figure A-4. Pulse transformer geometry

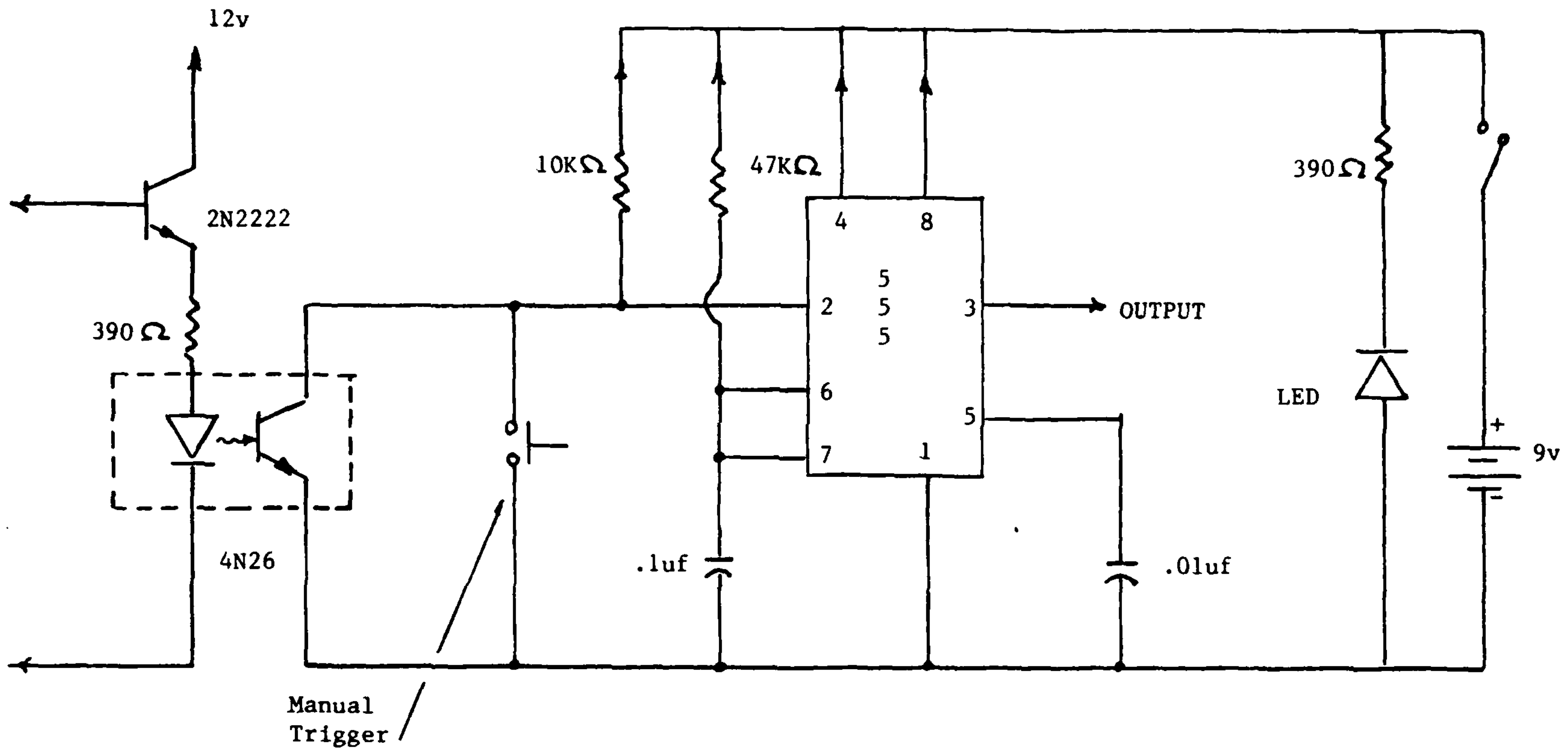

Figure A-3. Scope trigger circuit

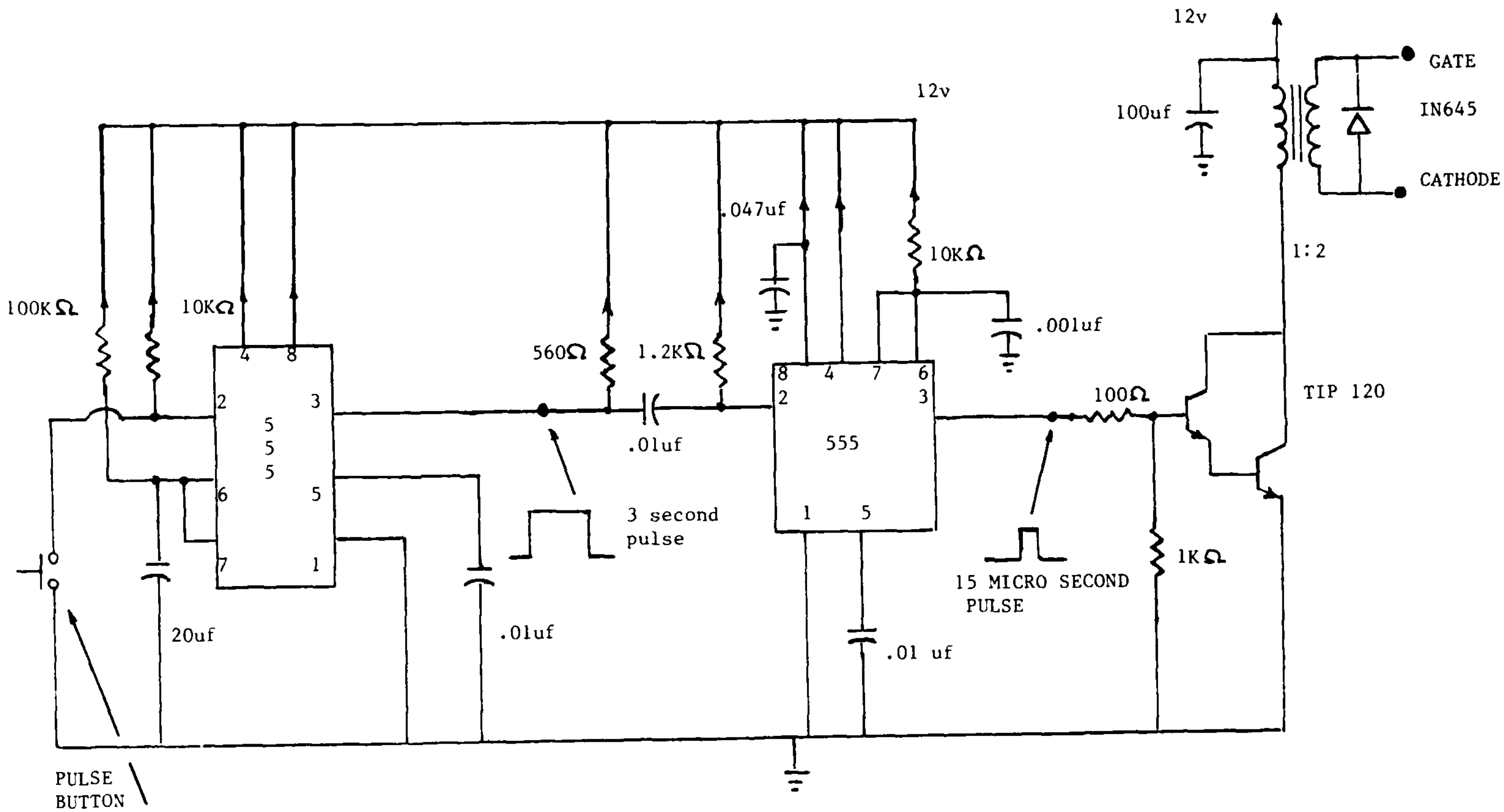

Figure A-2. SCR trigger circuit

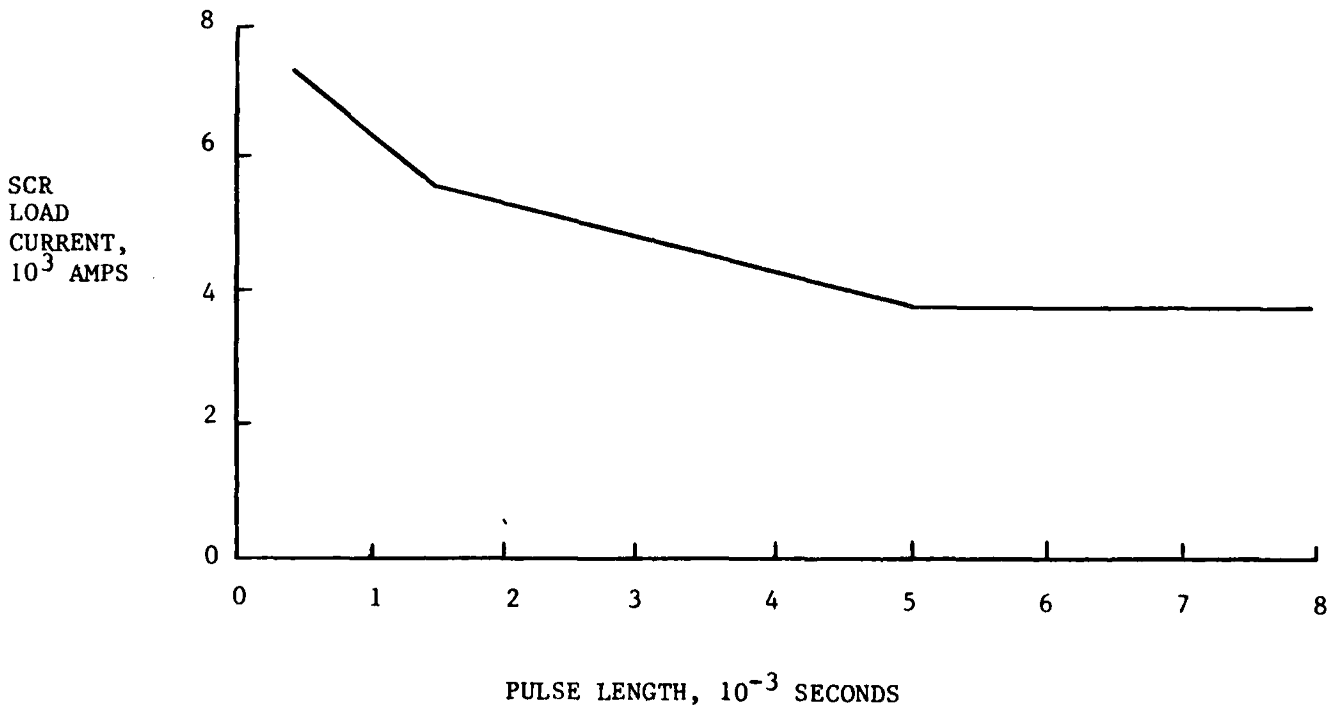

Figure A-1. Maximum SCR load current versus current pulse width

APPENDIX

SUPPLEMENTARY INFORMATION

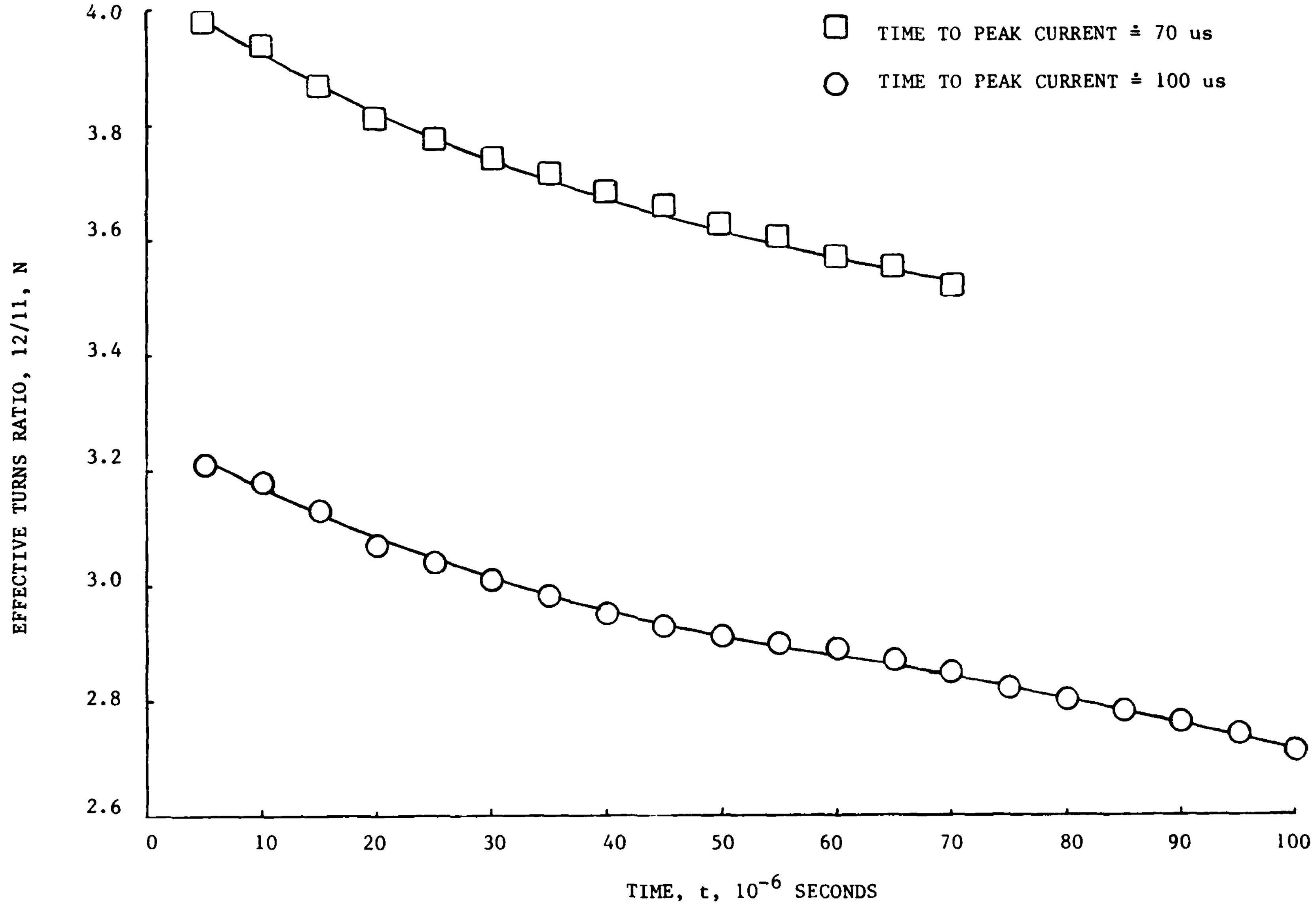

Figure 7. Turns ratio versus time

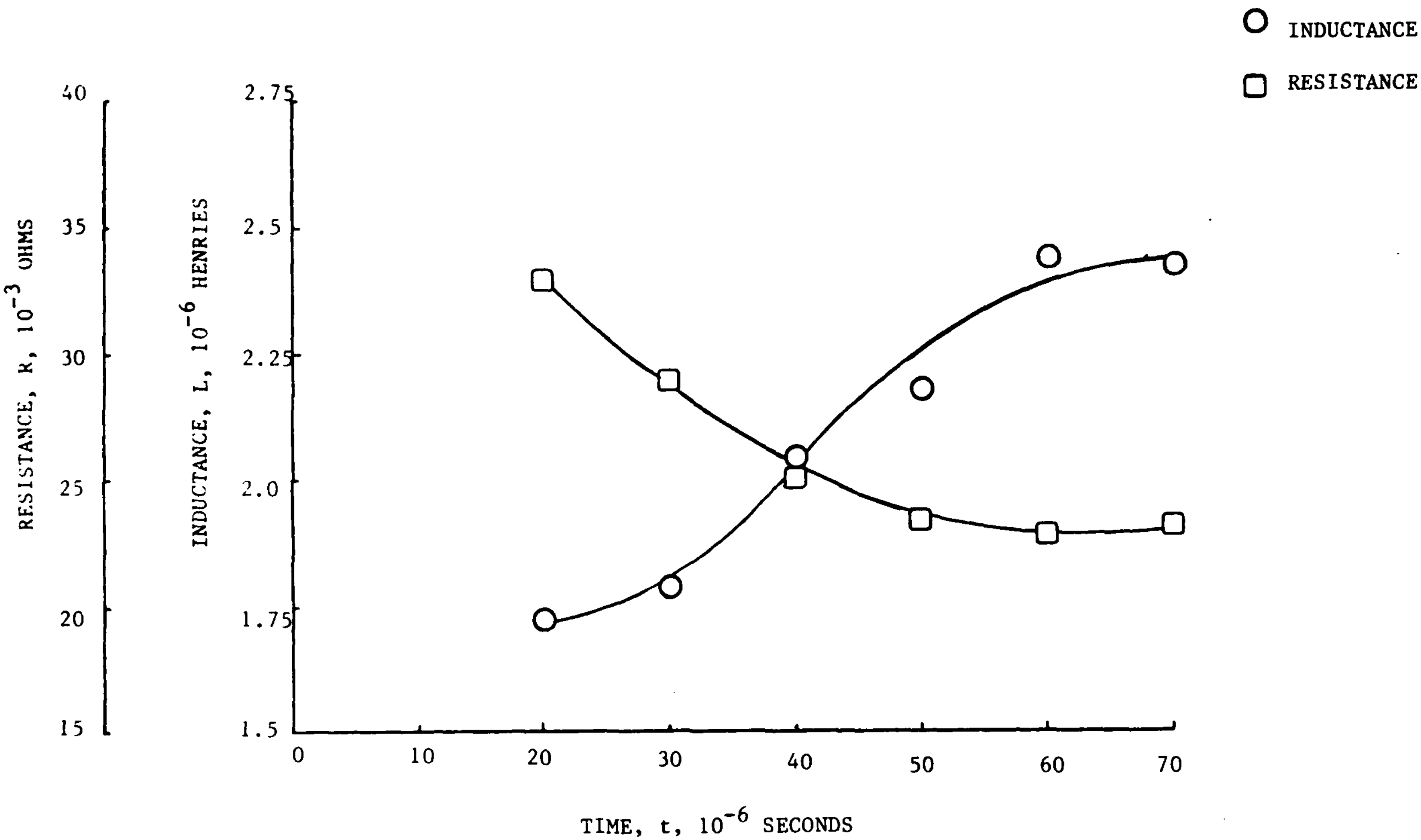

Figure 6. Pulse transformer inductance and resistance versus time

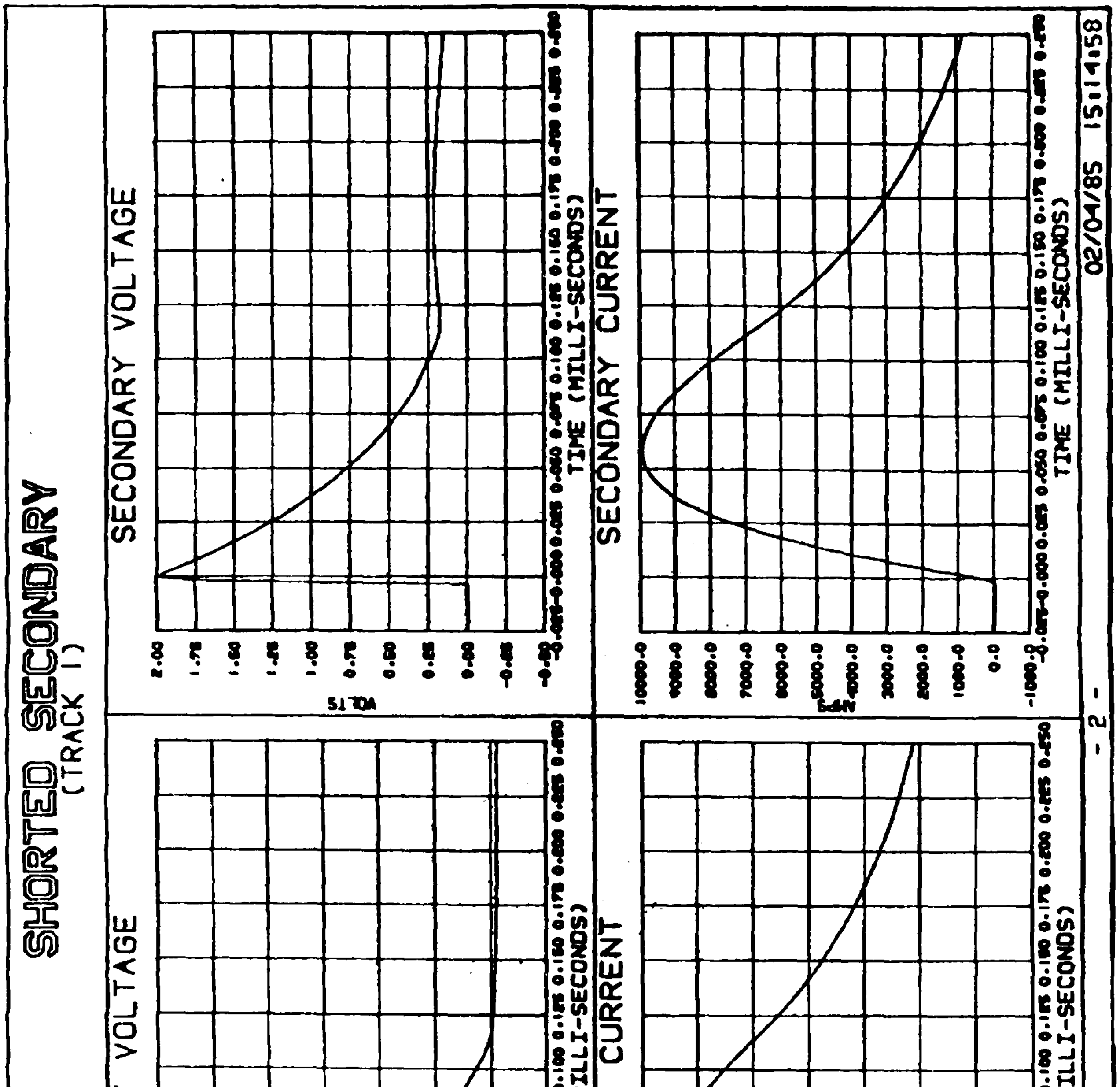

Figure 5. Test discharge with shorted secondary

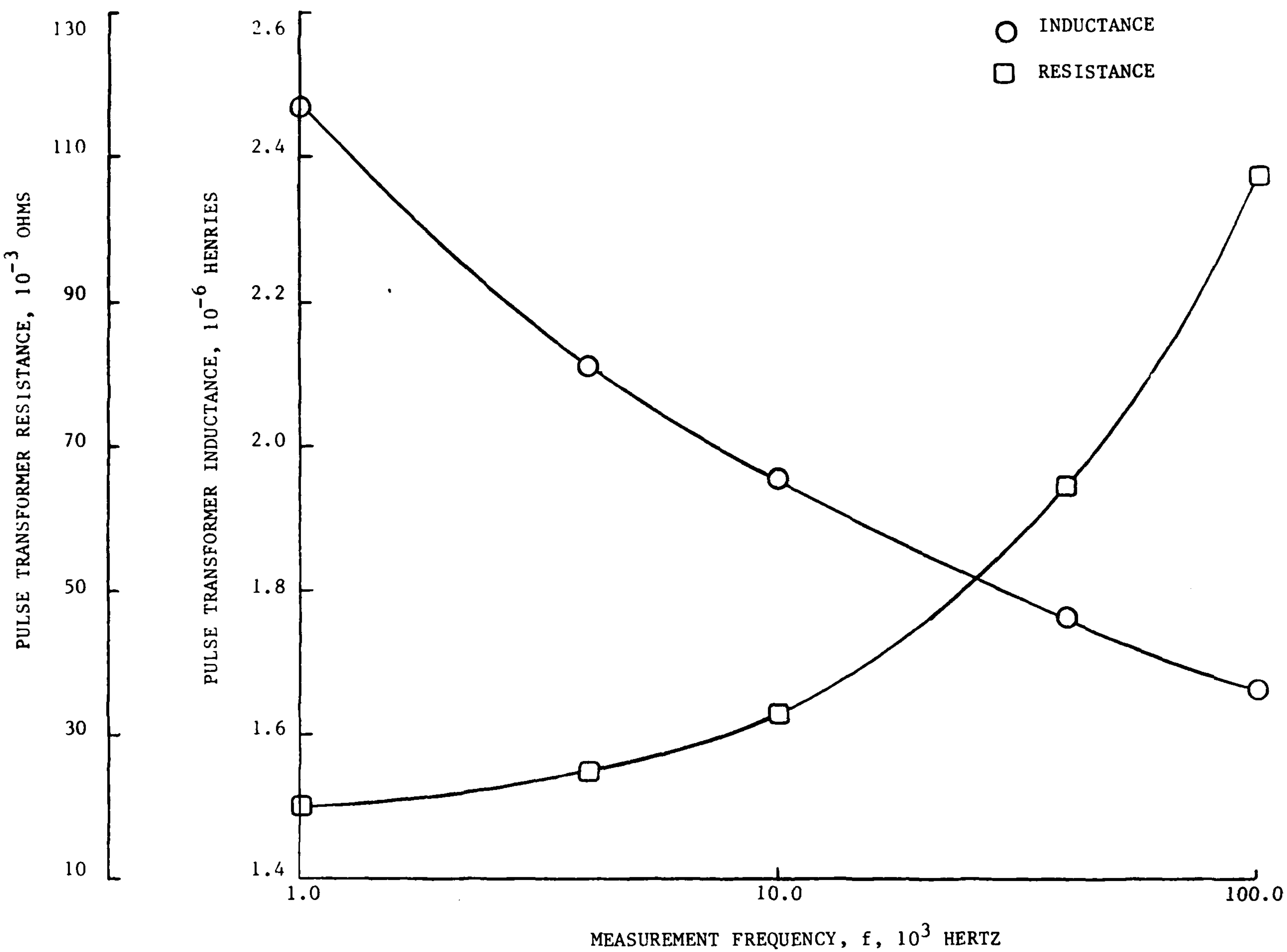

Figure 4. Pulse transformer measured input inductance and resistance versus frequency

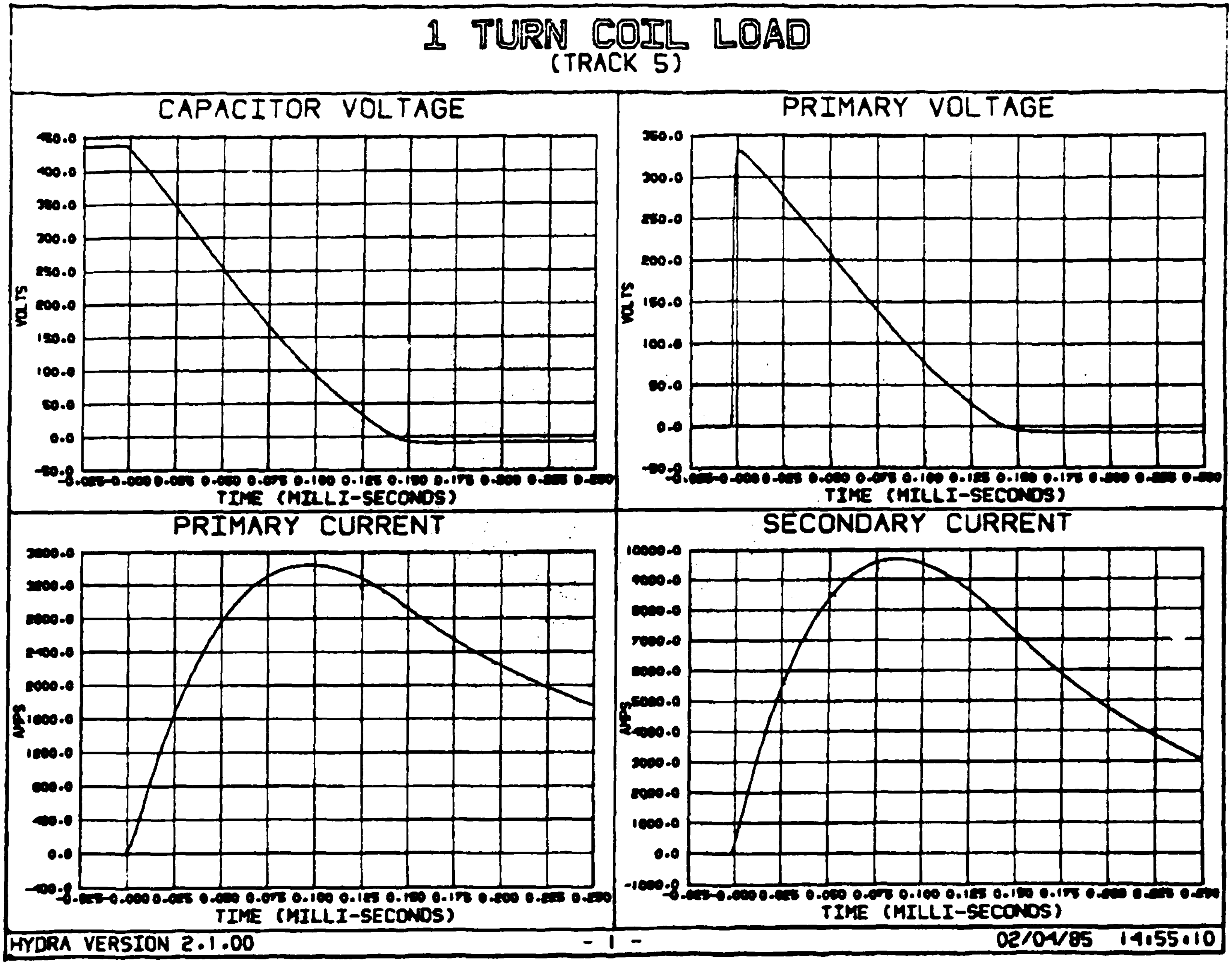

Figure 3. Test discharge with load coil connected

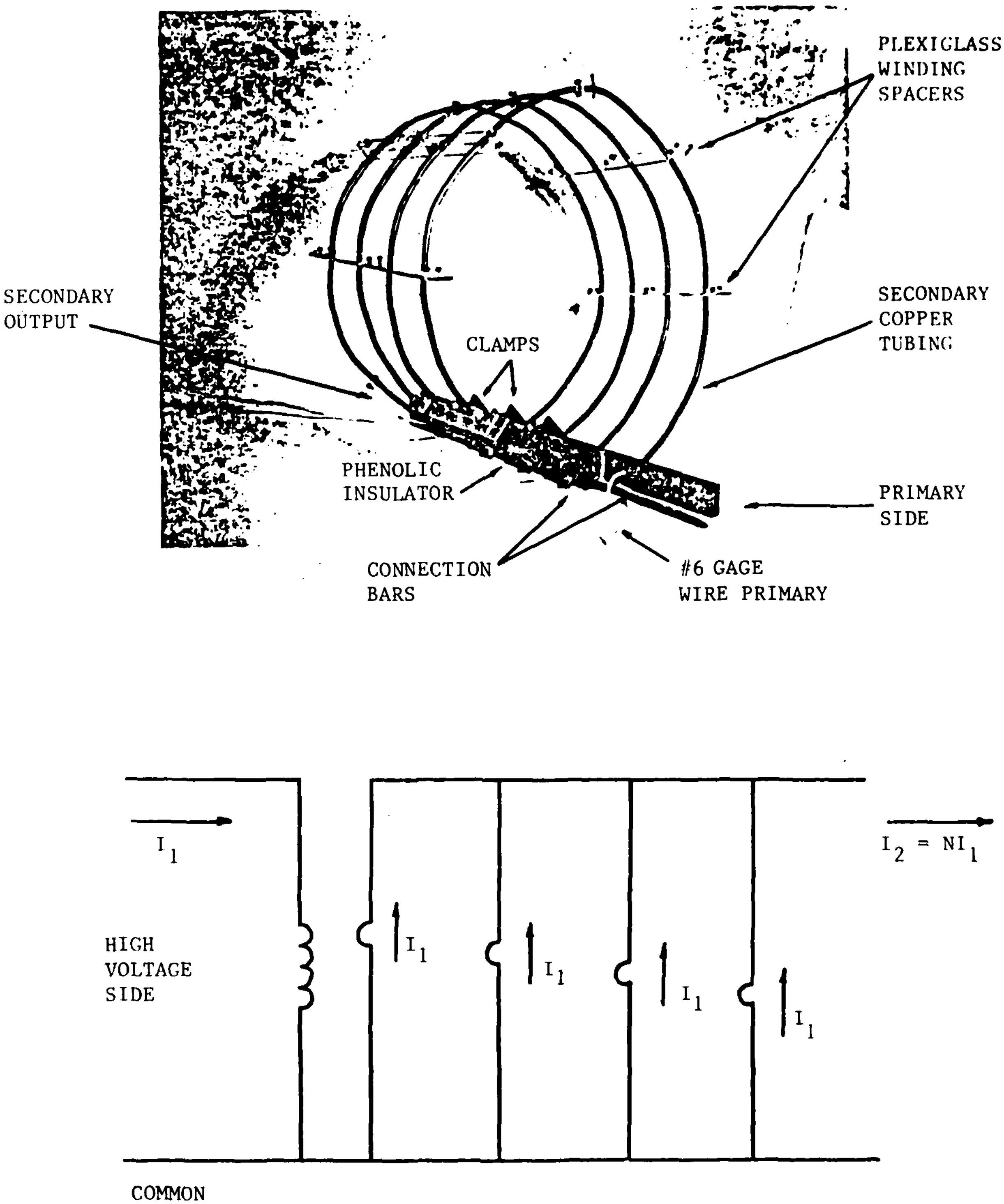

Figure 2. Pulse transformer and equivalent circuit